SCIENCE CHINA
Information Sciences

• LETTER •

May 2024, Vol. 67, Iss. 5, 159401:1–159401:2
https://doi.org/10.1007/s11432-023-3960-6

Enhanced fatigue resistance of ferroelectric $Al_{0.65}Sc_{0.35}N$ deposited by physical vapor deposition

Yang LI[1], Danyang YAO[1*], Yan LIU[1], Zhi JIANG[1], Ruiqing WANG[1], Xu RAN[1], Jiuren ZHOU[2], Qikun WANG[3], Guoqiang WU[4] & Genquan HAN[1,2*]

[1]*School of Microelectronics, Xidian University, Xi'an* 710071*, China;*
[2]*Hangzhou Institute of Technology, Xidian University, Hangzhou* 311200*, China;*
[3]*Ultratrend Technologies Inc., Hangzhou* 311199*, China;*
[4]*Emerging Device and Chip Laboratory, Institute of Technological Sciences, Wuhan University, Wuhan* 430072*, China*

Received 11 September 2023/Revised 25 November 2023/Accepted 19 February 2024/Published online 24 April 2024

Aluminum scandium nitride (AlScN), a III-V ternary semiconductor, has been recognized as an innovative and promising ferroelectric material in emerging research. Among the characteristics of ferroelectric material, fatigue resistance is a critical measure of the endurance of ferroelectric films and represents an inherent challenge in the pursuit of practical applications. For instance, ferroelectric random-access memory (FeRAM) is a non-volatile memory technology capable of reliable data reading, erasing, and rewriting over prolonged periods without failure [1, 2]. Accordingly, the fatigue resistance of ferroelectric materials directly influences the lifetime of FeRAM devices. However, the current maximum operational cycles observed in AlScN reach only up to 3×10^5 [3], significantly falling short of commercial requirements [4]. To address this issue, various attempts have been made using different material preparation methods [5].

In this study, we fabricated a robust ferroelectric AlScN film using the PVD method. The pure c-axis oriented ferroelectric phase was confirmed through x-ray diffraction rocking curve scans, even at a high scandium (Sc) concentration. The test results revealed that the fabricated AlScN ferroelectric capacitors can exhibit excellent polarization switching and retention capabilities. More importantly, the endurance of AlScN ferroelectric film was significantly improved to cross the milestone of ten million cycles for the first time. This work contributes to providing significant solutions for the development of more reliable non-volatile memory devices.

Figure 1(a) presents the key process steps for fabricating AlScN ferroelectric capacitor. The process begins with an AlN/Si template. Initially, a 150 nm thick Pt bottom electrode (BE) is sputtered onto the substrate. A 450 nm thick AlScN film is then deposited using custom-built sputter deposition equipment. Subsequently, after the deposition of the AlScN film, a top electrode (TE) consisting of a 5 nm thick Ti layer followed by a 95 nm thick Au layer is formed using electron beam evaporation (EBE). A shadow mask is used during the evaporation process to define the square capacitors with dimensions of 200 μm × 200 μm and 90 μm × 90 μm. Finally, the fabricated capacitors are ready for comprehensive testing and characterization. Figure 1(b) shows the schematic representation of a prepared ferroelectric capacitor.

Figure 1(c) shows a cross-sectional scanning electron microscope (SEM) view of the capacitor device. Figure 1(d) displays the high-resolution X-ray diffraction high resolution X-ray diffraction (HRXRD) 2θ-θ scan curve, and the (0002) reflection peak of AlScN is observed at 35.8° in 2θ. The inset in Figure 1(d) shows the ω rocking scan of the AlScN (0002) peak, which exhibits a full width at half maximum (FWHM) value of 2.28°. The presence of a c-axis preferred orientation, indicated by the absence of additional wurtzite peaks associated with other orientations, ensures the ferroelectric characteristics of the AlScN film. In the XPS results shown in Figure 1(e), the presence of Sc is detected through Sc 2p peaks at 406.5 eV. The Sc concentration, indicated by the Sc/(Al+Sc) ratio, is estimated to be approximately 35%, revealing a relatively high concentration of Sc.

Figure 1(f) shows the P-E loops obtained using a standard method. To mitigate interference from non-ferroelectric charge, a positive-up-negative-down (PUND) measurement pulse sequence is employed, which consists of four monopolar triangle voltage pulses. This pulse sequence is specifically designed to separate the contributions from both ferroelectric switching and non-ferroelectric switching components. The P-E and J-E loops of the $Al_{0.65}Sc_{0.35}N$ capacitors using the PUND method are then collected, as shown in Figures 1(g) and (h). The remnant polarization starts to saturate when the voltage exceeds 160 V, and the maximum remnant polarization is 143 μC/cm^2.

To investigate the frequency response of polarization switching, the ferroelectric capacitors with a small footprint of 90 μm × 90 μm were selected. These capacitors are anticipated to have a short RC delay time, making them more suitable for fast response. Figure 1(i) illustrates the measured frequency-dependent J-E loops, demonstrating that polarization switching can persist up to 15 kHz ($t_T \approx 33$ μs). Figure 1(j) illustrates the retention behavior of the capacitor. The test results indicate minimal or no decay in remnant polarization in both positive and negative directions

* Corresponding author (email: dyyao@xidian.edu.cn, gqhan@xidian.edu.cn)

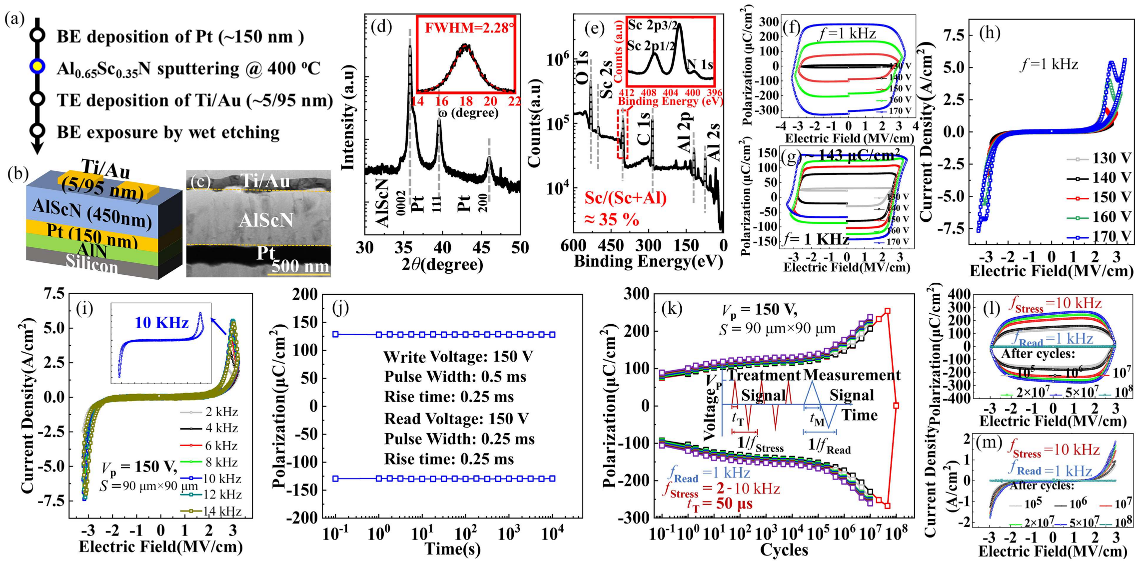

Figure 1 (Color online) (a) Key process steps for fabricating AlScN ferroelectric capacitor; (b) schematic representation of capacitor; (c) cross-sectional SEM view of the device indicating the thicknesses of AlScN as 450 nm; (d) HRXRD of the deposited AlScN/Pt/AlN/Si stacks. Inset shows the ω rocking curve of the material with FWHM of 2.28°; (e) XPS survey scan of AlScN thin film with a binding energy range of 0–600 eV. Inset: enlarged XPS survey scan of Sc 2p, N 1s; (f) measured P-E of the $Al_{0.65}Sc_{0.35}N$ capacitors collected with a triangular voltage pulse from 130 to 170 V at 1 kHz using standard method; (g) measured P-E of the $Al_{0.65}Sc_{0.35}N$ capacitors collected with a triangular voltage pulse from 130 to 170 V at 1 kHz using PUND method; (h) corresponding J-E loops using PUND method; (i) measured frequency dependent J-E loops up to 15 kHz; (j) retention behavior measurement; (k) measured remnant polarization during the fatigue tests for $Al_{0.65}Sc_{0.35}N$ capacitors with dimension of 90 μm × 90 μm; (l) measured P-E loops after fatigue treatments; and (m) the corresponding J-E loops.

over the entire testing duration of 10^4 s.

The devices were subjected to pulses with fixed t_T = 50 μs, V_p = 150 V for fatigue treatment. To monitor the degradation of the ferroelectric properties, measuring voltage pulses with f = 1 kHz, V_p = 150 V, but a longer t_M = 0.5 ms were introduced during the fatigue process. As illustrated in Figure 1(k), the fatigue tests conducted on ferroelectric capacitors with dimensions of 90 μm × 90 μm, demonstrate endurance beyond 10^7 cycles. Different colors represented samples from the same wafer, tested with frequencies increasing from 2 to 10 kHz with a step of 1 kHz. To explore the limits of endurance properties, fatigue training pulses with f = 10 kHz, t_T = 50 μs, and V_p = 150 V were continuously applied until degeneration occurred, reaching a final endurance of up to 5×10^7. Figures 1(l) and (m) show the measured P-E and J-E loops during the fatigue tests. At 10^8 cycles, remnant polarization and current density abruptly drop, indicating the almost complete disappearance of ferroelectric polarization. In fact, the degradation of AlScN capacitors involves the degradation of the ferroelectric phase, an increase in resistivity, and then a breakdown. In our case, the enhancement in a crystalline phase, along with the relatively thick films, allows us to observe the intermediate process of the degradation of the ferroelectric phase, rather than the breakdown phenomenon.

Conclusion. In summary, our study has achieved successful growth of a ferroelectric $Al_{0.65}Sc_{0.35}N$ film using the PVD method. The fabricated capacitors have demonstrated a coercive field of 2.70 MV/cm as well as an impressively large remnant polarization of 143 μC/cm^2. Significantly, we have set a benchmark by achieving a remarkable 5×10^7 switching cycle without observable substantial degradation. This advancement represents a promising way to enhance fatigue resistance, which could push forward the practical applications of this technology in non-volatile, low-power, intelligent, and reconfigurable electronics.

Acknowledgements This work was supported by National Natural Science Foundation of China (Grant Nos. 62025402, 62090033), Major Program of Zhejiang Natural Science Foundation (Grant No. DT23F0402), and Fundamental Research Funds for the Central Universities (Grant No. ZYTS23030).

References

1 Cross J S, Kim S H, Wada S, et al. Characterization of Bi and Fe co-doped PZT capacitors for FeRAM. Sci Tech Adv Mater, 2010, 11: 044402

2 Francois T, Grenouillet L, Coignus J, et al. Demonstration of BEOL-compatible ferroelectric $Hf_{0.5}Zr_{0.5}O_2$ scaled FeRAM co-integrated with 130nm CMOS for embedded NVM applications. In: Proceedings of IEEE International Electron Devices Meeting (IEDM), 2019. 1–7

3 Wang P, Wang D, Vu N M, et al. Fully epitaxial ferroelectric ScAlN grown by molecular beam epitaxy. Appl Phys Lett, 2021, 118: 223504

4 Pawlaczyk C Z, Tagantsev A K, Brooks K, et al. Fatigue, rejuvenation and self-restoring in ferroelectric thin films. Integr Ferroelectr, 1995, 9: 293–316

5 Mikolajick T, Slesazeck S, Mulaosmanovic H, et al. Next generation ferroelectric materials for semiconductor process integration and their applications. J Appl Phys, 2021, 129: 100901